

Localized Multiscale Texture Based Retrieval of Neurological Image

Sidong Liu¹, Lei Jing¹, Weidong Cai¹, Lingfeng Wen^{1,2}, Stefan Eberl^{1,2}, Michael J Fulham^{1,2,3}, Dagan Feng^{1,4}

¹ Biomedical and Multimedia Information Technology (BMIT) Research Group, School of Information Technologies, University of Sydney, Australia

² Department of PET and Nuclear Medicine, Royal Prince Alfred Hospital, Sydney, Australia

³ Sydney Medical School, University of Sydney, Australia

⁴ Centre for Multimedia Signal Processing (CMSP), Department of Electronic & Information Engineering, Hong Kong Polytechnic University, Hong Kong

Abstract

The volume and complexity of neurological images have significantly increased, which leads to challenges in efficient data management and retrieval. In this paper, we developed a new content-based image retrieval framework with the localized multiscale Discrete Curvelet Transform (DCvT) features extracted from parametric neurological images. We also compared the performance of three different irregular-to-regular shape padding methods. 142 patient data with neurodegenerative disorders were used in the evaluation. The preliminary results show that our proposed framework supports fast neuroimaging retrieval, and the orthographic projection method can reduce the computational complexity and has a great potential to improve the retrieval for indefinite cases.

1. Introduction

Neuroimaging is essential for the accurate diagnosis of neurological disease. The anatomical imaging techniques of Magnetic Resonance (MR) imaging and Computed Tomography (CT) are the main imaging modalities used in the neurosciences for the evaluation of suspected structural lesions including stroke, tumors and demyelination. Functional imaging such as positron emission tomography (PET), however, offers the ability to identify functional changes before there are anatomical imaging changes. This capability underscores its increasing relevance in the evaluation of neurodegenerative disorders such as the dementias. Advances in instrumentation and the introduction of combined devices such as PET-CT offer the opportunity for further refinements in neuroimaging diagnosis. These advances have also substantially increased the volume of imaging data and posed challenges for the efficient management and retrieval

of such imaging data. Traditional retrieval methods, mainly based on text-searches, are limited; they are not able to take advantage of the rich visual / physiological information in the images. Therefore, Content-based image retrieval (CBIR) methods were proposed to provide fast and reliable image retrieval [1].

A number of CBIR systems for neurological images have been reported. Wong *et al.* [2] presented a neuro-informatics database system (NIDS) for co-registered PET-MR images, using the mixture of geometric location information, metabolic counts of glucose consumption and text annotations in the image file header. Betty *et al.* [3] designed a prototype system for PET neuroimaging retrieval with regions of interest (ROI) that were segmented using the Talairach and Tournoux atlas. The texture features were extracted through Gabor filters and then combined with a related mean index ratio, which measured the scale difference between whole brain metabolic activity and ROI metabolic activity. Both these teams of investigators used raw PET uptake images and did not take account of the uptake time and injected dose of individual patients [2, 3].

We proposed a CBIR approach for functional metabolic neuroimaging based on the cerebral metabolic rate of glucose consumption (CMRGlc) [4]. In its application to neurodegenerative disease, we proposed a set of disorder-oriented masks (DOM) to facilitate image retrieval. These DOMs were initially created with clinical expertise and then refined by the *t-map* [5].

Our recent investigation in the retrieval of general images using DCvT has suggested that DCvT is an effective tool in capturing edges and singularities along curves in images, and has a great potential for textured image retrieval [6]. We now propose a new CBIR approach that uses the DCvT-based texture features to enhance image retrieval and investigate the performance using clinical patient data in this study.

2. Methods

2.1. Neuroimaging Data Preprocessing

Raw static PET data were pre-processed in two steps, deriving CMRGlc images and atlas-based spatial normalization. In the first step, parametric images of CMRGlc were constructed from original raw static FDG ([18F] 2-fluoro-deoxy-glucose) PET images using the autoradiographic (ARG) algorithm [7].

Spatial normalization eliminated the inconsistencies between individuals in size and scan orientation and aided image interpretation among multiple subjects. The CMRGlc images were transformed with the SPM2 package [8] to the MNI (Montreal Neurological Institute) space, which has standardized dimensions of 91 x 109 in 91 planes. The spatially normalized CMRGlc images were labeled according to the Tzourio-Mazoyer atlas [9], which is based on the MNI single subject template. The Tzourio-Mazoyer atlas defines 45 functional regions in each hemisphere, 18 regions in cerebellum and 8 regions in cerebellar vermis.

2.2. Adaptive Disorder-Oriented Mask (DOM) Construction

We defined a set of initial DOMs, each of which corresponded to one type of dementia, based on clinical expertise. The initial DOMs were further refined by the *t-map*, which is a parametric image derived by voxel-by-voxel comparing individual value with the mean value and standard deviation of a number of age-matched control subjects. The pixel values in a CMRGlc image were first translated into values in a standard normal distribution. For a given threshold ($p\text{-value} < 0.05$), the abnormal values compared with age-matched controls were retained with other values set to zero. If the regions with a non-zero value of *t-map* were not included in the initial DOMs, the regions were added to the corresponding DOMs [4].

Each DOM contained a subset of the functional regions defined in the Tzourio-Mazoyer atlas. Figure 1 gives an example of the DOMs for Alzheimer's disease (AD) and frontal-temporal dementia (FTD) across different planes. Initially, the DOM for AD contained 37 regions of the Tzourio-Mazoyer atlas. *T-map* refinement added 8 more functional regions.

2.3. Multiscale Texture Feature Extraction

The Curvelet transform is a multiscale image representation approach developed by Candes and

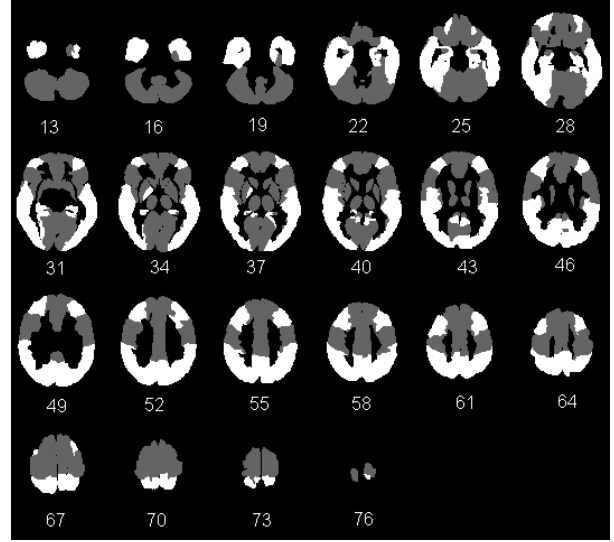


Figure 1. a) The DOM for AD in different planes.

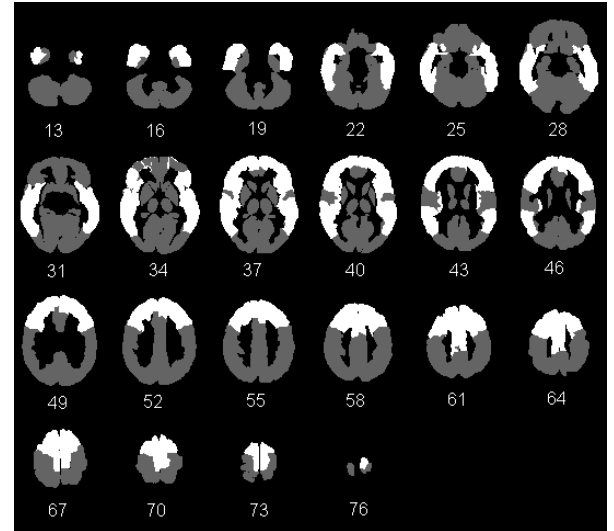


Figure 1. b) The DOM for FTD in different planes.

Donoho [10]. The features based on continuous Curvelet transforms (CCvT) are superior to traditional texture feature descriptors, such as wavelet, ridgelet and Gabor filters [10-12]. Based on CCvT, Candes *et al.* further proposed the digital Curvelet transform (DCvT) for providing a simpler, faster and more accurate construction operation on digital data [13]. Curvelet transforms require the regions to be rectangular. However, as shown in Figure 1, the regions' shapes are highly irregular in neurological images. Therefore, the feature extraction process was completed in two stages, the rectangular reshaping followed by DCvT-based feature extraction.

2.3.1. Irregular to Regular Shape Padding. We evaluated three reshaping methods to transform the irregular image contours to rectangles. First, we used a zero-padding technique to fill the positions of the non-region pixels in the full sized images, with uniform dimensions of 91 x 109.

The second method was background cropping followed by zero-padding [14]. The background accounted for a large part of the images thus including a large amount of noise. To cut off the background, we identified the smallest outer rectangle for the real content. Then we extracted it and put zeros to non-region pixels, as shown in Figure 2.

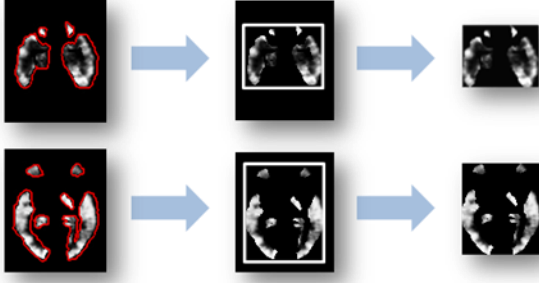


Figure 2. Background cropping.

Without any DOM, a patient case contained 91 planes. Applying the DOMs can lower the number of planes and the DOM for FTD may decrease the number of planes to 65. Method 3 used orthographic projection to further reduce the dimension. This approach considered the entire case as a volume and used three planes to represent it. As shown in Figure 3, the three projected images can represent the whole volume without losing information contained in small fractions while preserving the curvilinear information of larger areas.

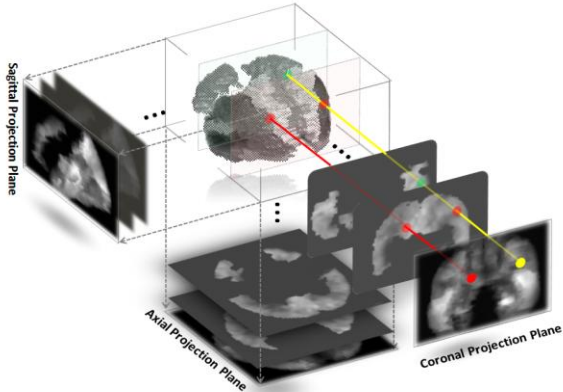


Figure 3. Orthographic projection.

2.3.2. Optimized Localized DCvT-Based Texture Feature Extraction. For a given image/plane $f(x)$, where $x = (x_1, x_2)$, a Curvelet transform can be defined by the scale parameter j , translation parameter k , and orientation parameter l as follows:

$$\varphi_{j,l,k}(x) = \varphi_j(R_{\theta_l}(x - x_k^{(j,l)})) \quad (1)$$

$\theta_l = 2\pi \cdot 2^{\lfloor -j/2 \rfloor} \cdot l$, where $l = 0, 1 \dots$ satisfying $0 \leq \theta_l \leq 2\pi$. $k = (k_1, k_2) \in \mathbb{Z}^2$ and $x_k^{(j,l)} = R_{\theta_l}^{-1}(k_1 \cdot 2^{-j}, k_2 \cdot 2^{-j/2})$. R_{θ_l} is the rotation by θ_l radians. Then a Curvelet coefficient is the inner product between an element $f \in L^2(\mathbb{R}^2)$ and a Curvelet $\varphi_{j,l,k}$:

$$c(j, l, k) : \langle f, \varphi_{j,l,k} \rangle = \int_{\mathbb{R}^2} f(x) \overline{\varphi_{j,l,k}(x)} dx \quad (2)$$

The DCvT is based on Cartesian arrays transformed from the frequency coroneae of CCvT. Assuming the image has a dimension of $n \times n$, take $f[t_1, t_2]$ as input, DCvT outputs a set of discrete coefficients:

$$CvT^D(j, l, k) := \sum_{0 \leq t_1, t_2 < n} f[t_1, t_2] \overline{\varphi_{j,l,k}^D[t_1, t_2]} \quad (3)$$

The DCvT can be implemented by Unequally Spaced Fast Fourier Transform (USFFT) approach or the Wrapping algorithm [13]. Wrapping algorithm supports periodic tiling and could be simpler to understand and implement. Therefore, we used the Wrapping-based method to perform the Curvelet transforms.

In our recent study [6], we evaluated the performance of the full range of Curvelet transform scales and found that it offered the best results at 3-scale and 12-angle in the second coarsest level by using the second level coefficients only. In this paper, we applied the same approach to extract the features of our dataset. The mean and standard deviation of the selected Curvelet transform coefficients were computed to construct the feature vectors. If m Curvelets were used, a feature vector would contain $2m$ elements. Due to the symmetry property of the Curvelet transform, only half of the 12 sub-bands Curvelets in the selected level were used.

3. Performance Evaluation

We used the query by example paradigm in this study. The retrieval was conducted by the leave-one-out strategy on the whole dataset. The similarity was calculated using Euclidean distance and the performance was evaluated by the average precisions versus number of images retrieved curves [15].

We evaluated our approaches on the patient dataset which contained 142 functional neurological cases taken in the Royal Prince Alfred Hospital. It included

38 AD cases (Male: 17, Female: 21, Age: 51-73), 37 FTD cases (Male: 21, Female: 16, Age: 53-74), 37 cases of other disorders (Male: 19, Female: 18, Age: 50-75) and 18 normal cases (Male: 11, Female: 7, Age: 53-75). A special group (AD/DLBD) which comprised 12 ‘indefinite’ cases (Male: 5, Female: 7, Age: 55-73) was also included in the database. These 12 cases were claimed ‘indefinite’, because they exhibited the neurodegenerative patterns of both AD and Diffuse Lewy Body Disease (DLBD). Taking the ROI overlap between these disorders into consideration, the relevance criteria setting for different disorder classes are listed in Table 1.

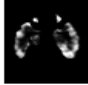
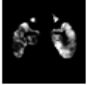



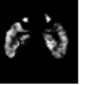

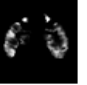
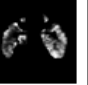
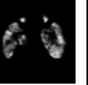
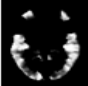



















Table 1. Criteria for measurement of relevance.

| Score | Criteria |
|-------|---|
| 1.0 | The retrieval image belongs to the class of the query image |
| 0.75 | For indefinite disorders, the retrieval image belongs to either class which the query images related to |
| 0.25 | The retrieval result belongs to any disorder class other than the classes it belongs or relates to |
| 0.0 | The retrieved image belongs to normal class |

Here we introduced a new similarity measurement method based on the distance between corresponding planes. For any two cases, e.g. P_A and P_B , we first selected the i^{th} plane of all n planes, and then calculate the distance, d_{AB_i} , between the i^{th} plane in P_A and the corresponding plane in P_B . The distance from P_A to P_B is then defined as follows:

$$D_{AB} = \sum_{i=1}^n d_{AB_i} \quad (4)$$

Table 2. Top 10 retrieval results of a query case.

| Patient ID Plane NO. | AD: P00424 | AD: P06225 | AD: P02680 | DLBD: P05590 | AD: P08782 | AD: P02226 | AD/DLBD: P11998 | DLBD: P09815 | AD: P01660 | AD: P12013 |
|-------------------------|---|---|---|---|---|---|--|---|---|---|
| Distance | 0.0000 | | | | | | | | | |
| Plane 25 |  |  |  |  |  |  |  |  |  |  |
| Plane 40 |  |  |  |  |  |  |  |  |  |  |
| Plane 55 |  |  |  |  |  |  |  |  |  |  |
| Overall Distance | 0.0000 | 64.3727 | 65.7100 | 66.5120 | 67.0580 | 69.2151 | 69.3062 | 69.6549 | 69.9467 | 70.8455 |

4. Results

We tested our approaches on three disorders, AD, FTD and AD/DLBD. Table 2 shows an example of top 10 retrieval results of an AD query, using the zero-padding technique on full sized images. The first column was the query case.

Four different texture features were extracted from one case. As labeled in Figure 4. ‘DOM_AD/FTD’ indicates that the DOM for either AD or FTD was applied on the full sized images to extract the features; ‘*_Cropping’ means the features were extracted from the background cropped images; ‘*_Projection’ represents features extracted from the projected images, and ‘Global’ stands for the whole-brain-based features.

Figure 4 shows the comparison of our proposed three approaches and the whole brain based approach. From the curves, we found that the DOMs could greatly facilitate the neuroimaging retrieval. In all three disorder groups, especially the AD group, DOM-based approaches indicated by the dashed lines outperformed the whole-brain-based approach indicated by the solid lines. The curves also demonstrated that features based on full sized images and cropped images yielded very similar results. In AD and AD/DLBD groups, only a slightly better result was achieved by the approaches based on full sized images than the approaches based on cropped images. In addition, the performance of using projection technique was higher than the other approaches in AD/DLBD group, while in the other two groups, similar performance was found. When comparing the results across all the three disorder groups, we found that the retrieval performance for AD was much better than that of the other two.

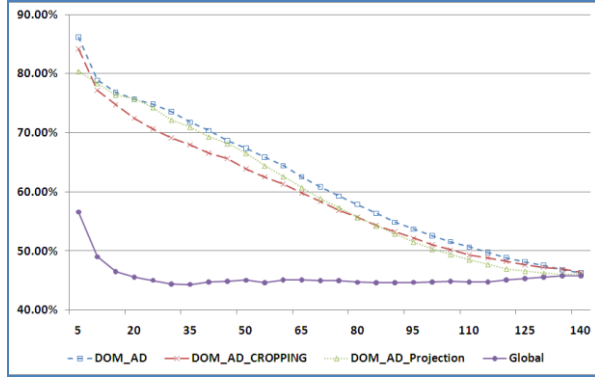


Figure 4 a). Average precision versus number of retrieval results curves for AD cases.

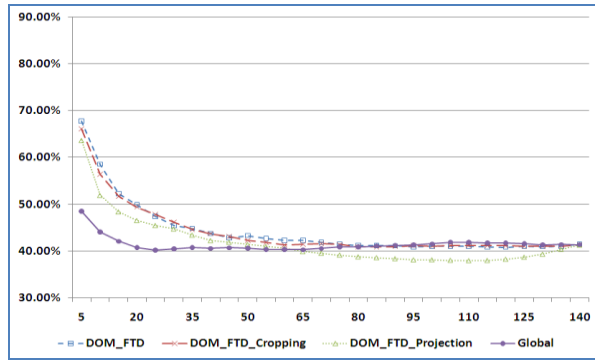


Figure 4 b). Average precision versus number of retrieval results curves for FTD cases.

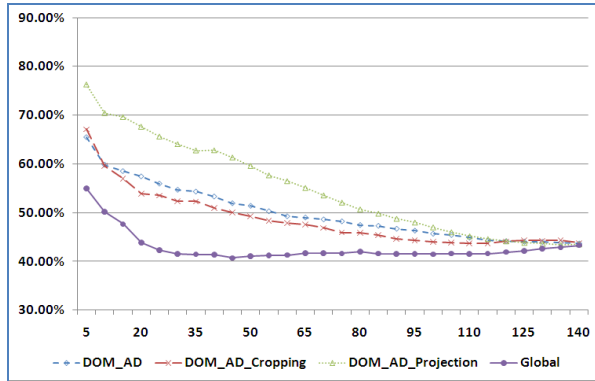


Figure 4 c). Average precision versus number of retrieval results curves for AD/DLBD cases.

5. Discussion

Different from traditional 2D image retrieval, we did not use individual planes as the search entities. Instead, we considered the patient case as a whole. That means the query we used was an entire case containing multiple planes. A widely used method is

to use one single feature vector to represent the entire case by averaging the vectors of all the planes. However, this method might bring a lot of noise caused by the small fractions and flatten the significance of single planes. Our corresponding plane-based distance measurement method will not compromise the significance of individual planes because only the difference between corresponding planes will be counted in the distance calculation. In addition, the corresponding plane-based method will not be affected by the discrepancy of the dimensions of different cropped planes. In Figure 2, we can see the cropped images have different sizes, but the corresponding planes were having the same dimensions, and they were not compared to other planes with different dimensions.

Our approaches could reduce the computational complexity in two ways. First, the dimension of the feature vector in our study was very small when compared with the vectors used in other studies with tens or hundreds of elements. Second, the projection approach used only three planes to represent the multiple planes. It greatly reduced the number of planes yet achieved comparable performance with other approaches.

There were some findings indicated by our experiment results. Full sized images and cropped images yielded very similar results. This was because the cropping process only changed the image sizes, but did not bring more information of the curvilinear properties. We also found that the projection method was robust in AD and FTD groups, and brought much better result in AD/DLBD group. This implied that the projection technique might enhance the obtained texture features for indefinite AD/DLBD group.

6. Conclusions

In this paper, we proposed a CBIR approach based on optimized Curvelet features. Our approach greatly reduces the computational complexity and supports fast neuroimaging retrieval. The improvements in performance by using DOMs are well demonstrated and the largest improvement is observed in AD group. For all three disorder groups, the approach of using background cropping technique cannot bring better results than the non-cropping approach. However, the projection approach has a great potential to improve the retrieval for AD/DLBD cases.

7. Acknowledgment

This work was supported in part by ARC and PolyU grants.

References

- [1] H. Muller, N. Michoux, D. Bandon, and A. Geissbuhler, "A review of content-based image retrieval systems in medical applications – clinical benefits and future directions", *International Journal of Medical Informatics*, vol.73, pp.1-23, 2004.
- [2] S.T.C. Wong, K.S. Hoo, X. Cao, D. Tjandra, J.C. Fu, and W.P. Dillon, "A neuroinformatics database system for disease-oriented neuroimaging research", *Academic Radiology*, vol.11, no.3, pp.345-358, 2004.
- [3] S. Batty, J. Clark, T. Fryer, and X. Gao, "Prototype system for semantic retrieval of neurological PET images", *The International Conference on Medical Imaging and Informatics (MIMI 2007)*, Aug 14-16, 2007, Beijing, LNCS 4987, pp.179-188, 2008.
- [4] W. Cai, S. Liu, L. Wen, S. Eberl, M.J. Fulham and D. Feng, "3D neurological image retrieval with localized pathology-centric CMRGlc patterns", *The Int. Conf. on Image Processing (ICIP 2010)*.
- [5] S. Liu, W. Cai, L. Wen, S. Eberl, M.J. Fulham and D. Feng, "A robust volumetric feature extraction approach for 3D neuroimaging retrieval", *The 32nd Int. Conf. of IEEE Eng. in Med. and Biol. Society (EMBC 2010)*.
- [6] L. Jing, W. Cai, D. Feng, "Texture based image retrieval using optimized multiscale Curvelet transform", *The 10th Asian Conference on Computer Vision (ACCV2010)*, submitted for publication.
- [7] S. Eberl, A.R. Anayat, R. Fulton, P.K. Hooper, and M.J. Fulham, "Evaluation of two population-based input functions for quantitative neurological FDG PET studies", *European Journal of Nuclear Medicine*, vol.24, no.3, pp.299-304, 1997.
- [8] R. Frackowiak, K.J. Friston, C.D. Frith, *et al.*, *Human Brain Function*. Amsterdam; Boston: Elsevier Academic Press, 2004.
- [9] N. Tzourio-Mazoyer, B. Landeau, D. Papathanassiou, *et al.*, "Automated Anatomical Labeling of Activations in SPM Using a Macroscopic Anatomical Parcellation of the MNI MRI Single-Subject Brain", *NeuroImage*, vol.15, no.1, pp. 273-289, 2002.
- [10] E. J. Candes and D. L. Donoho, "Curvelets – a surprisingly effective nonadaptive representation for objects with edges", *Curves and Surfaces*, pp.105-120, Vanderbilt University Press, Nashville, TN, 2000.
- [11] L. Dettori, L. Semler, "A comparison of wavelet, ridgelet and Curvelet based texture classification algorithms in computed tomography", *Computers in Biology and Medicine*, vol.37, pp.486-498, 2007.
- [12] I. J. Sumana, M. M. Islam, D. Zhang and G. Lu, "Content based image retrieval using Curvelet transform," *The Proc. of Int. workshop on MMSP*, Oct, 2008.
- [13] E. J. Candes *et al.* "Fast Discrete Curvelet Transforms", *Multiscale Modeling and Simulation*, vol. 5, no.3, pp. 861-899, 2006.
- [14] M. Islam, D. Zhang, G. Lu, "Region based color image retrieval using Curvelet transform", *The 9th Asian Conference on Computer Vision (ACCV2009)*.
- [15] M LLER, H., M LLER, W., SQUIRE, D. M., MARCHAND-MAILLET, S. & PUN, T, "Performance evaluation in content-based image retrieval: overview and proposals," *Pattern Recognition Letters*, vol.22, pp.593-601, 2001.